Scalable convergent synthesis of therapeutic oligonucleotides

Xianglin Shi (xianglin.shi@biogen.com)
Biogen https://orcid.org/0000-0001-9512-7570
Xuan Zhou
Biogen https://orcid.org/0000-0002-6412-7655
Wuming Yan
Biogen
William Kiesman
Biogen Inc https://orcid.org/0000-0003-2910-0008
Yannick Fillon
Biogen
Hong Jiang
Biogen
Firoz Antia
Biogen https://orcid.org/0000-0001-7960-4277
Li Xiao
Biogen
Jing Yang
Biogen
Armin Delavari
Biogen
Robert Gronke
Biogen

Article

Keywords: oligonucleotides, phosphoramidite approach, PO/PS

Posted Date: August 6th, 2021

DOI: https://doi.org/10.21203/rs.3.rs-594481/v1

Scalable convergent synthesis of therapeutic oligonucleotides

Xuan Zhou†, Wuming Yan†, William F. Kiesman, Yannick A. Fillon, Hong Jiang, Firoz D. Antia, Li Xiao, Jing Yang, Armin Delavari, Robert S. Gronke, Xianglin Shi*

Antisense Oligonucleotide (ASO) Process Development, Biogen, Cambridge, MA 02142, USA

*Correspondence to: xianglin.shi@biogen.com

†These authors contributed equally to this work.

Abstract. The recent explosive growth in the number of oligonucleotide clinical development programs and drug approvals underscores their ability to treat diseases via mRNA regulation. Currently, solid-supported synthesis is limited to ≤ 5 kg (~ 1 mole) batch sizes and the feasibility of liquid-phase syntheses to supply materials of sufficient purity and amount for clinical trials has not been proven. Herein we describe the first convergent synthesis of a full-length 18-mer mixed backbone (PO/PS) 2'-MOE gapmer oligonucleotide by the phosphoramidite approach suitable for use in clinical trials. Techniques described to control impurities during its synthesis can be implemented in common active pharmaceutical ingredient (API) manufacturing facilities and should enable a >10-fold increase in production batch scaling.

Messenger RNA (mRNA) has increasingly become a therapeutic target.[1, 2] Therapeutic oligonucleotides regulate the composition and quantity of mRNAs through splicing regulation, RNase H-mediated degradation, or RNA interference mechanisms [3-5] with downstream effects on protein expression. Eleven chemically synthesized oligonucleotide drugs have been approved to treat rare diseases,[2, 6] which include antisense oligonucleotides (ASOs) and small interfering RNAs (siRNAs) made via solid-phase oligonucleotide synthesis (SPOS). In current clinical research, new oligonucleotides are showing great promise to treat diseases afflicting millions of people, including cardiovascular disease, and yearly demand for each drug could reach over a metric ton. [2]

The current SPOS process at ~ 5 kg scale [7] would require ~200 batches to deliver 1000 kg. While it is conceivable that economies of scale may be realized in massive, specialized facilities, this approach has significant engineering and cost challenges [8] as well as a negative environmental impact. [9]

An alternative approach is the development of an economical liquid-phase oligonucleotide synthesis (LPOS) that can be carried out in existing synthetic API manufacturing plants. The most advanced efforts reported in the literature use linear synthesis strategy similar to SPOS (Fig. 1A) by building the oligonucleotide chain on soluble polymeric anchors [10] that enable the simplification of intermediate isolations by using precipitation and extraction extractions. Separation of the intermediates via membrane filtration based on an homostar anchor has also been reported (Fig. 1B).[11] To date, feasibility of LPOS of a typical therapeutic oligonucleotide has not been

demonstrated beyond a few grams at a time, although linear synthesis of morpholino oligonucleotides has been reported at a 10-kg scale.[10]

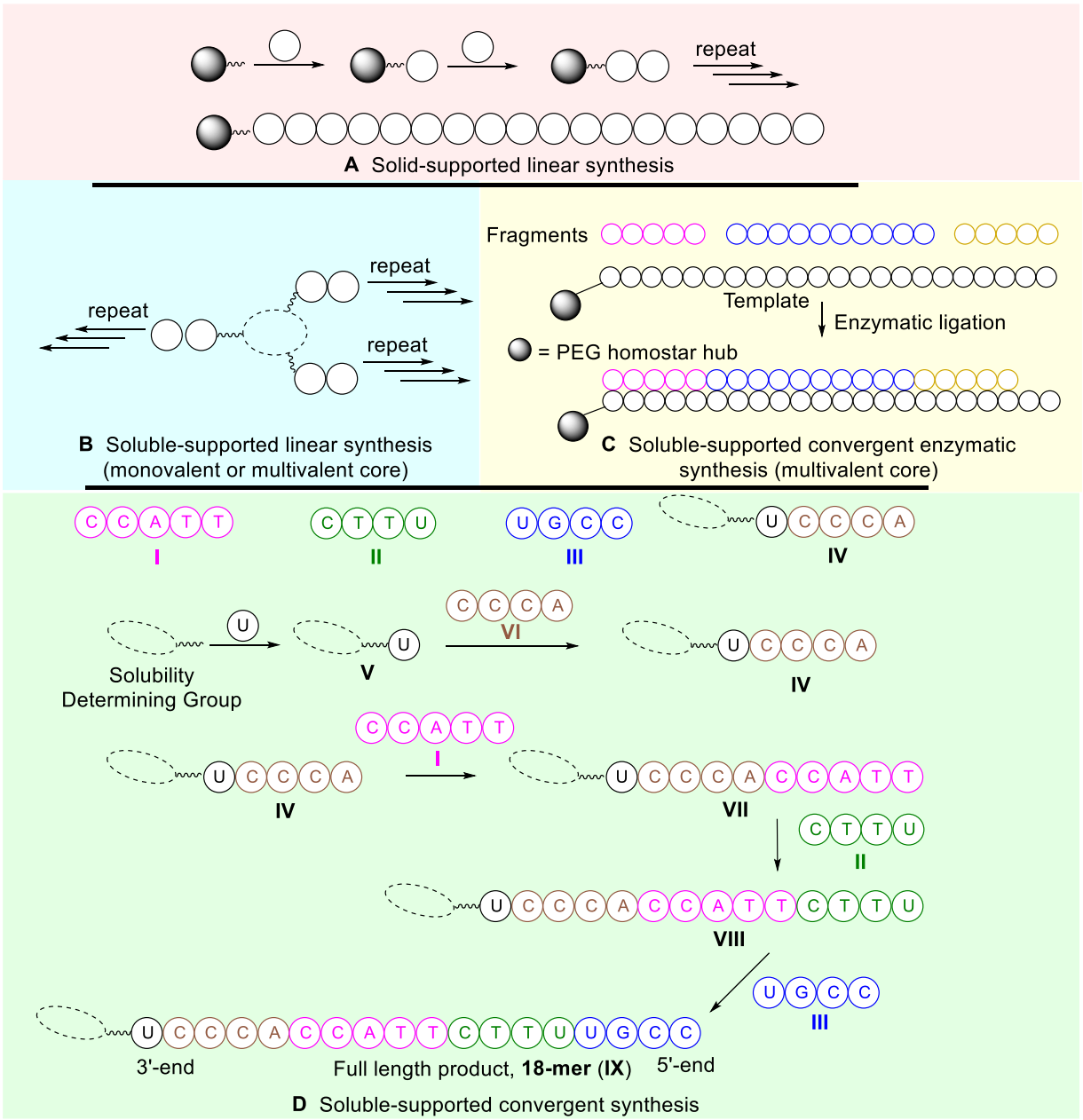

Figure 1. Synthetic strategies for oligonucleotide synthesis

Only a few literature examples describe convergent oligonucleotide syntheses. Among them are the synthesis of a 6-mer assembled from phosphoramidites,[12] a 37-mer from phosphotriesters,[13] a 21-mer employing *H*-phosphonates,[14] a 20-mer by a template-guided enzymatic assembly (Figure 1C),[15] and double-stranded siRNAs by enzymatic synthesis.[16] Unlike-phosphonates and phosphotriesters, many phosphoramidites suitable for the synthesis of therapeutic oligonucleotides are commercially available. To date, enzymatic reactions have only worked efficiently for the synthesis of natural phosphodiester (PO) bonds and broadening the technology to phosphorothioate (PS) linkages that are dominant in ASO and siRNA therapeutics [17] has had limited success. Furthermore, product analyses of the alternative approaches to SPOS reported rely heavily on liquid chromatography with UV detection (LC-UV). [18, 19] This technique is insufficient to resolve and quantify all of the product related impurities.[20] Therefore, it is difficult to know whether they will provide oligonucleotides with purities high enough to support clinical trials. [21, 22] Quantitation of certain types of product related impurities can currently only be achieved by LC-UV coupled to mass spectrometry (LC-UV-MS). [23] Herein, we report the chemical learnings and characterization details from the development of a scalable convergent LPOS (Fig. 1D) of an 18-mer oligonucleotide **ON-A** by the phosphoramidite approach that provides a product with purity comparable to that made from the current state-of-the-art SPOS. The sequence of **ON-A** is 5'- $^{Me}C^{Me}C_oG^{Me}U^{Me}UTT^{Me}CTTA^{Me}C^{Me}CA^{Me}C_o^{Me}C^{Me}C^{Me}U$-3', where red = 2'-O$(CH_2)_2OCH_3$ (MOE) nucleotides, and black=2'-deoxy ribose nucleotides; o indicates a phosphate (PO) linkage and the remaining are phosphorothioate (PS) linkages; Me indicates 5-methyl in C and U.

Results and discussion

Synthetic Challenges and Strategic Approaches. A single strand of an ASO or siRNA typically contains 18 to 25 nucleotides and requires up to 100 separate chemical reactions to synthesize, as installation of each nucleotide proceeds via a four-reaction cycle. [7, 23, 24] To scale up the synthesis of therapeutic oligonucleotides, impurities must be controlled to very low levels in each isolated intermediate to avoid accumulation of impurities that cannot be separated from the full-length product (FLP) during purification. The majority of existing LPOS strategies require extensive purification of intermediates by precipitation,[25] extractions, [26] or chromatography.[27]

Time consuming isolations with accompanying product losses and large solvent requirements can be reduced by telescoping the coupling, sulfurization, and detritylation reactions in each cycle. [28, 29] The full-length **ON-A** may be assembled convergently (Fig. 1D) from 2 tetramer (**II** and **III**) and 2 pentamer (**I** and **IV**) fragments. This approach can be expected to provide significant operational, economic, and quality advantages over the linear syntheses including:

1. shorter production cycle time with parallel processing of fragments
2. reduced product isolation losses
3. reduction in impurities- as nucleotides are exposed to fewer reaction cycles and are less likely to degrade and or participate in undesired side reactions
4. more effective impurity purging from smaller intermediate fragments
5. limited impact of single batch failure with independent fragment synthesis

For the full-length **ON-A** synthesis, tetramers and pentamers of deoxy and MOE fragments **I-IV** (Fig. 2A) were made separately. The free 3'-OH in fragments **I-III** was converted into the corresponding phosphoramidites prior to coupling with the 5'-OH of the fragment **IV**, **10-mer**

(**VII**), or **14-mer** (**VIII**). Synthesis of the Solubility Determining Group (SDG)-containing fragment **IV** can be accomplished by growing the full fragment from SDG-nucleotide **V** or by coupling of **V** with fragment **VIa**. SDG (MW~ 1000 Da) [19] is a protecting group that imparts the overall solubility of each fragment.

Attempts to control the impurity burden across the entire process focused on 1) using extremely dry reaction conditions to avoid deamination impurity formation during detritylations; 2) implementing use of a novel thiol DMTr cation scavenger to achieve > 99.95% detritylation with simultaneous suppression of retritylation during work-up; 3) achieving >99.95% coupling reaction completion with minimal amidite excess by rigorous drying of reaction solutions; 4) complete removal of the difficult to remove byproduct amidite derivatives, by exploitation of the relative solubility differences between impurities and intermediates or fragments; 5) separation of the fragments **I**-**III** from **VII**-**IX** during full-length assembly by use of the SDG installed in fragment **IV**; 6) use of a 3'-OH protecting group that is stable during synthesis and removed quantitatively following fragment assembly.

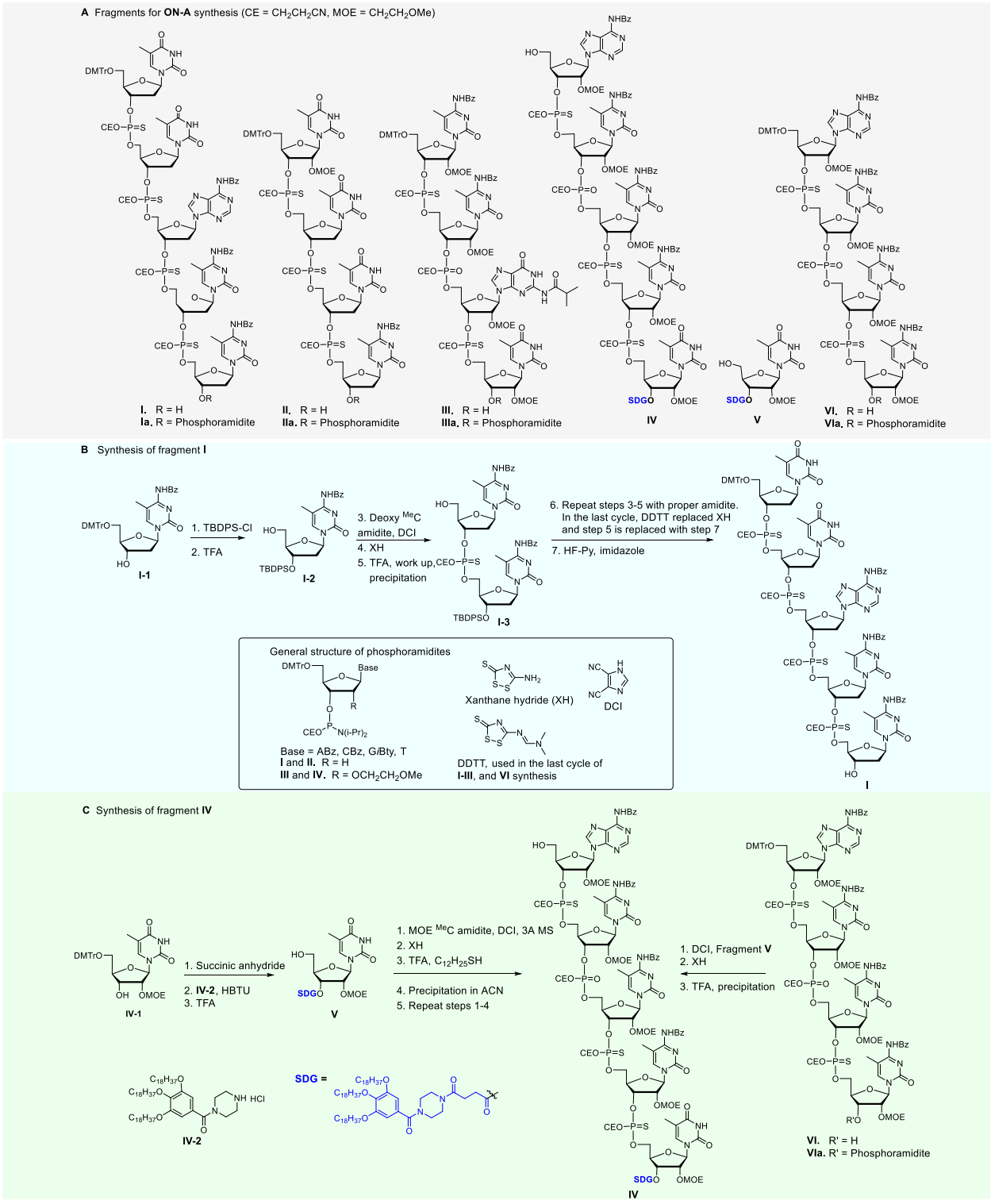

Figure 2. Fragments for convergent synthesis of ON-A and synthesis of fragment I and IV

Synthesis of I-IV. Syntheses of **I-III** and **VI** started with 3'-OH protection of the first nucleoside with TBDPS-Cl followed by detritylation to provide the 3'-OTBDPS nucleosides (for example, see compound **I-2** in the synthesis of **I** (Fig. 2B)). A DCI mediated coupling of **I-2** with deoxy ^{Me}C amidite followed by sulfurization with xanthane hydride (XH) and detritylation with TFA in one pot provided dimer **I-3**. Fragment **I** was synthesized by repeating this procedure with required amidites, except that in the last cycle 3'- OTBDPS deprotection, rather than the 5'-ODMTr detritylation, was performed. Synthesis of **II-III** and **VI** followed the same reaction cycle under similar conditions, except for two cycles where oxidation rather than sulfurization was performed to install the PO linkages. The coupling reactions produce chirality at the phosphorus P(III) stereocenter. The stereoselectivity of the coupling reaction is determined mainly by the amidites, their coupling partners and the activator.[30-32] DCI was used as an activator to maintain similar stereochemistry in both the LPOS and SPOS processes. Solvents were chosen to enable telescoping with high reaction efficiency and work-up simplicity. Rigorous residual water control (<100 ppm) and reaction monitoring (HPLC) enabled > 99.95% reaction completions using 1.05 (for the first cycle) to 1.4 (for the last cycle) equivalents of the amidite starting materials, which is less half of the amidites when compared to prior literature examples.[25, 28]

XH was used for sulfurizations for all but the last cycle in **I-III** and **VI** syntheses since its byproduct was found to promote detritylation. Consequently, DDTT was used in the last cycle. In the trimer synthesis for **III** and **VI**, I_2/pyridine was used to introduce the PO linkages. Isolations were performed after the oxidation since the large quantity of pyridine used made the one-pot reaction impractical. For PS/PO mixed backbone fragments, a one-pot oxidation reaction using *m*-

Cl-$PhCO_2H$ [28] resulted in high PO impurities; alternatively, use of *t*-BuOOH led to difficult to remove coupling products of amidites and *t*-BuOH.

Dichloroacetic acid (DCA) is commonly used for SPOS detritylations; however, trifluoroacetic acid (TFA) was found to be more effective in LPOS and produced fewer impurities. In addition, use of thiols, novel DMTr cation scavengers, significantly reduced the equivalents of TFA (~7) and reaction times (~30 min at 0 ^{o}C). Without added thiols, reactions stalled even with 20 equivalents of TFA. Retritylation observed during work-ups was eliminated when thiol use was increased to 3.0 equivalents. In the last cycle of the synthesis of **I**-**III** and **VI** the detritylation was replaced with a 3'-OTBDPS deprotection reaction, which was accomplished with a novel HF-imidazole combination. This was the only deprotection condition that gave clean and facile reactions, while the typical literature conditions afforded complex mixtures at reaction completion.

After the detritylation or desilylation (last cycle) reaction of the one-pot synthesis was complete, a work-up was carried out, which generally included quenching with aqueous $NaHCO_3$ solution, extraction, washing, and precipitation to remove impurities based on their solubilities. In the dimer syntheses using ^{Me}C, the amidite derivatives were removed by filtration through a SiO_2 pad, which retained the amidite derivatives.

The synthesis of **IV** was accomplished by two routes (Fig. 2C). The coupling of **V** with tetramer amidite **VIa** produced significantly lower n-1 impurities than the one-pot linear elongation [29] of **IV-1**. For full details on the optimized experimental conditions for the syntheses of all fragments please refer to the Supplementary Materials.

A

Fragments	I	II		III	IV[1]	VI	
Scale (kg/batch)	0.3	0.3	3	0.3	0.2	0.3	3
Yield (%)	72	59	76	73	77	68	62
Purity (%)	93.4	90.2	93.0	87.6	90.8	86.6	87.7
PO (%)	<0.10	0.70	0.11	0.59	0.87	<0.10	0.15
n-1 (%)	<0.10	0.16	0.44	1.1	0.15	0.29	0.27
Deamination (%)	<0.10	<0.10	<0.10	0.10	NT[2]	0.25	<0.10

[1] Fragment IV was analyzed after ammonolysis.
[2] NT = not tested

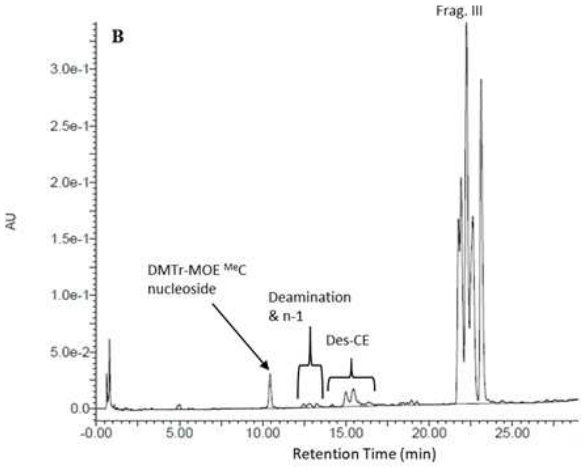

Figure 3. Fragment synthesis results. (**A**) Yield, purity, and common critical impurities of fragments **I-IV** and **VI.** (**B**) LC-UV chromatogram of fragment **III.**

The yield improvements in the larger scale preparation of fragment **II** (Figure 3A) were driven by improvements of the coupling reaction of each cycle that enabled the reduction of amidite excesses which subsequently lessened impurity burden and product loss in workups. The lower isolated yield for the kilo-scale synthesis of fragment **VI** (Figure 3A) was due to a vessel leak that resulted in the loss of ~ 17% monomer starting material solution during drying prior to the coupling reaction.

Impurities in fragments are considered critical if they lead to impurities in FLP that are not effectively removed by purification; all other impurities are non-critical.[33] Fig 3A shows that the critical impurities, including PO, n-1, and deamination, as determined by LC-UV-MS analysis, were controlled to low levels in all fragments. Most non-critical impurities are more polar and elute earlier than the fragments, as shown in the LC-UV chromatogram of fragment **III** (Fig 3B).

Loss of the cyanoethyl (CE) protecting group forms the Des-CE impurities (~4.6%), which are eventually converted into the desired FLP after convergent assembly and global deprotection. The other non-critical impurity observed at a relatively high level (~2%) is the DMTr-MOE ^{Me}C nucleoside originating from MOE ^{Me}C amidite used in the last cycle of fragment **III** synthesis.

Control of Impurities. Minimizing impurity generation is a key focus during development of a good pharmaceutical manufacturing process. It is even more critical in the synthesis of oligonucleotides due to their accumulation through a greater number of reactions. Several classes of impurities are formed during synthesis and each class contains multiple distinct impurities that can occur at various positions in the sequence (Fig. 4A).[21] The families of impurities formed

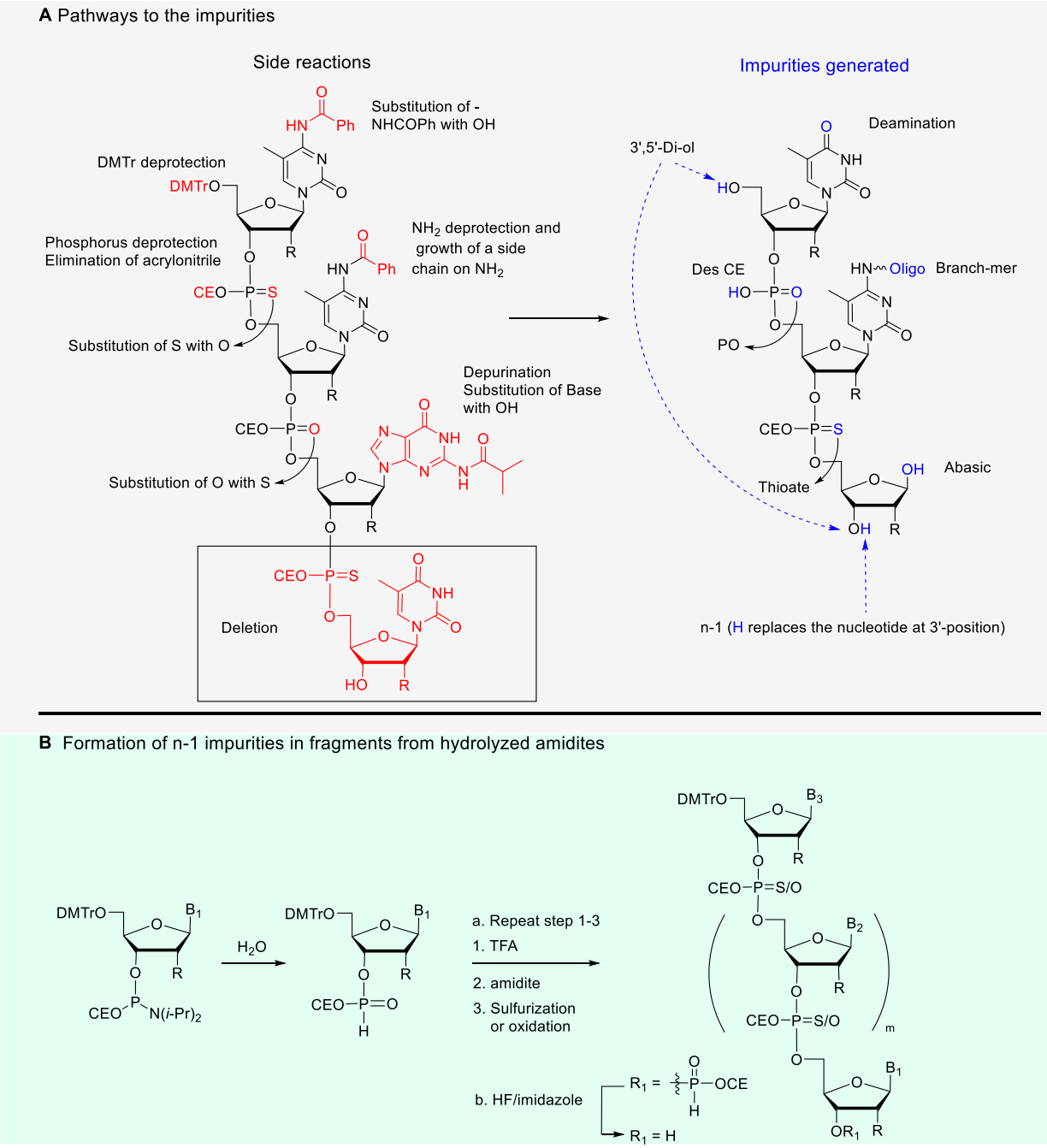

Figure 4. Main impurities and pathways for formation

during synthesis are the result of incomplete reactions leading to truncated n-1 impurities, over reactions generating extended n+1 impurities, and degradation reactions including hydrolytic replacement of the N^4-NHBz in the nucleobase C (deamination) and the nucleobase A and G from

the ribose (abasic), deprotection of amino (NH_2) groups contained in A and C that may lead to branched impurities, and sulfur substitution with oxygen (PO) or vice versa (thioate). The following discussion focuses on n-1 and deamination impurities, which are both easy to produce and difficult to control and remove during purification of the DMTr-on **ON-A** (**X**, Fig. 5).

Truncated n-1 impurities. The n-1 impurities can arise from incomplete coupling, sulfurization, or detritylation. Therefore, controls must be put in place for each reaction in each cycle. Due to the repetition of reaction cycles to grow an oligonucleotide, even 0.1% of an n-1 impurity from each of the 3 reactions in every chain-extension cycle can add up to a large impurity burden. For example, for an 18-mer **ON-A**, this would result in an unacceptable level of 5.4% n-1 impurities after 18 cycles.

With an incomplete coupling reaction, the remaining 5'-OH participates in the coupling of the next cycle and gives rise to an n-1 impurity. Capping unreacted 5'-OH is employed in SPOS [23] and some LPOS.[11] Alternatively, in LPOS syntheses coupling reactions are driven to completion by adding 3.0 equivalents of amidites [25, 28] to avoid the need for capping. Since amidites are expensive and their byproducts are challenging to remove from the intermediates, minimizing their use has an impact not only on process economics, but also on the process performance. We minimized n-1 impurities by achieving on average ≥ 99.95% coupling completion with 1.05 (cycle one) to 1.3 (cycle four) equivalents of amidites by drying the reaction mixture to < 100 ppm residual water using 3 Å molecular sieves. More amidite was required for later cycles as it proved difficult to reduce equivalents of residual water from the reaction solutions. No significant coupling reactivity difference was noticed in fragments of different lengths.

Incomplete sulfurization or oxidation reactions leave the newly attached nucleoside linked through an acid labile P(III) phosphite triester that can be cleaved during detritylation in the following cycle resulting in an n-1 impurity. Complete sulfurization and oxidation reactions are accomplished with XH or DDTT and I_2 as described previously.

Incomplete detritylation or its reverse reaction, retritylation, also leads to n-1 impurities. Primary thiols were found to be excellent DMTr cation scavengers that drive the deprotection to completion and prevent retritylation. In the presence of 3.0 equivalents of $C_{12}H_{25}SH$, the detritylation reaction reached >99.95% completion using 5 (cycle one) to 12 equivalents (in later cycles) of TFA with no detectable retritylation observed during the work-up. These conditions contrast with the 25-70 equivalents of Cl_3CCO_2H and 15-25 equivalents of Et_3SiH as a cation scavenger that were used to achieve reaction completion in Walther's procedure. [28]

The n-1 impurities can also arise from 3'-*H*-phosphonates, the hydrolysis products of excess amidites, present in the dimer intermediates. The *H*-phosphonate group acts as a 3'-OH protecting group and allows the chain to grow from the 5'-OH during fragment synthesis. Its removal from 3'-OH in the TBDPS deprotection step produces an n-1 fragment (Fig. 4B). This n-1 fragment eventually propagates into full-length n-1 impurity after the convergent assembly. The n-1 impurities from this pathway were controlled by limiting amidite excesses, adding aqueous washes, filtering through silica, or product precipitation.

Deamination impurities. A surprisingly significant side reaction of LPOS that is not usually observed in SPOS is the substitution of the N^4-NHBz of cytidines by -OH (Fig. 4A) during the

detritylation reaction at 0-22 ºC. This hydrolytic deamination product results in the conversion of ^{Me}C to T. In early LPOS syntheses >12% of ^{Me}C to T deamination impurities were observed in **IV**. A preliminary investigation indicated that these impurities likely formed under acidic condition by direct displacement of N^4-NHBz with residual H_2O. Also, the 5-methyl group, or a nucleotide attached either at 3' or 5' end, could significantly increase the reaction rate. Control of residual water in the reaction medium to < 100 ppm eliminated this side reaction and ensured very low levels of deamination impurities in all fragments.

Although reactions of N^4-acylcytidines under neutral condition at 125 ºC [34] and 1-methyl cytosine in refluxing 80% acetic acid [35] have been previously described, the hydrolytic deamidation under acidic conditions is not reported during SPOS. In earlier LPOS literature water has been added to enhance the detritylation reaction,[36] even with intermediates containing N^4-benzolylcytidines.[37] This LPOS data clearly highlight the significance of this side reaction in the detritylation reaction and all work-ups under acidic conditions, particularly for ASOs containing 5-^{Me}C.[38]

Assembly of the Full-Length ON-A. Full-length 18-mer **ON-A** was assembled by the same coupling, sulfurization and detritylation reaction cycles (Fig. 5). The fragment **I** was first converted into its amidite **Ia** by reacting with the phosphitylation reagent. Coupling of **Ia** with **IV** followed by sulfurization and precipitation from acetonitrile provided DMTr-on **VII**. Detritylation required ~13 equivalents of Cl_3CCO_2H, was completed in 1.5 h, and precipitation afforded **VII**. The precipitations removed fragment amidite **Ia** and its derivatives from the 10-mer product **VII**. An unoptimized one-pot process required about 25 equivalents of Cl_3CCO_2H and 3 h to complete. Repeating the coupling, sulfurization and precipitation, and detritylation (step excluded in the last

cycle) and precipitation, **VII** was converted into **VIII**, and then to fully protected **IX**. Phosphorus deprotection followed by global deprotection by heating with NH_4OH provided crude **X**.

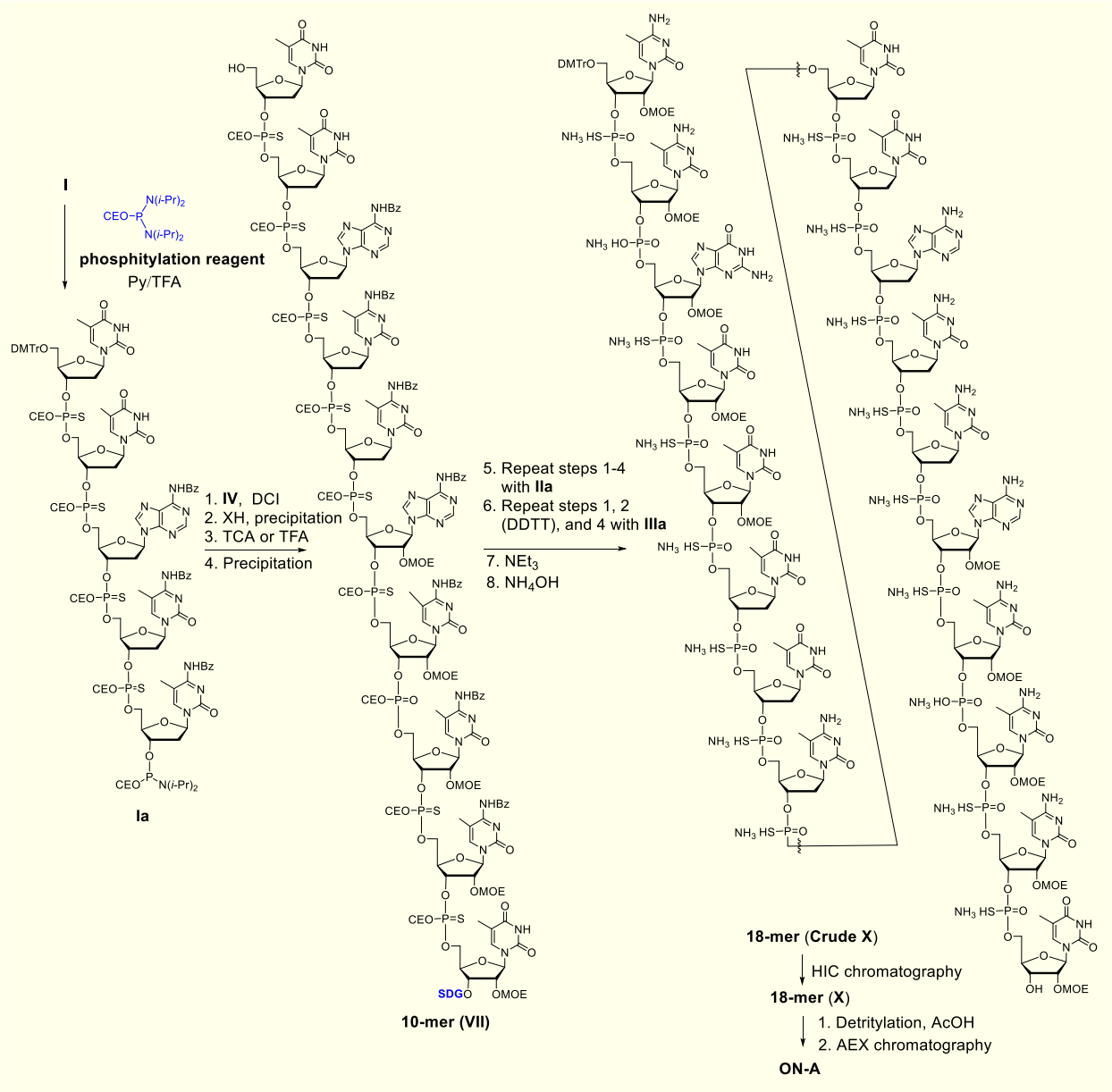

Figure 5. Convergent assembly of ON-A

Several side reactions were observed in the synthesis of amidites **Ia**-**IIIa** and **VIa** and assembly steps. Use of ≤2 equivalents of the phosphitylation reagent produced dimeric 8-mer and 10-mer derivatives of **I-III** and **VI**. Residual phosphitylation reagent in **Ia**-**IIIa** was also found to react with fragment **IV**, **VII**, and **VIII** in the coupling steps (Fig. 5) to generate the corresponding amidites that in turn generate dimeric impurities of **IV**, **VII** and **VIII**. In the coupling reactions > 99.0% conversions of **IV**, **VII** and **VIII** were achieved with 1.2, 1.3, and 1.4 equivalents of **Ia**-**IIIa**, respectively. Incomplete coupling, detritylation and sulfurization resulted in n-4 and n-5 impurities. Although these shortmer impurities could not be removed from the desired **VII**, **VIII**, and **IX** by precipitations, they were removed during purification and downstream processing, which used the same process as SPOS including hydrophobic interaction chromatography (HIC), detritylation, and AEX chromatography.

Impurity profiles of crude X and ON-A. Figure 6 shows the results of LC-UV-MS analysis of the crude **X** from convergent LPOS and SPOS and corresponding **ON-A** after the standard purification procedure. The FLP and impurities were quantified by LC-UV-MS analysis. The convergent LPOS produced crude **X** in lower overall

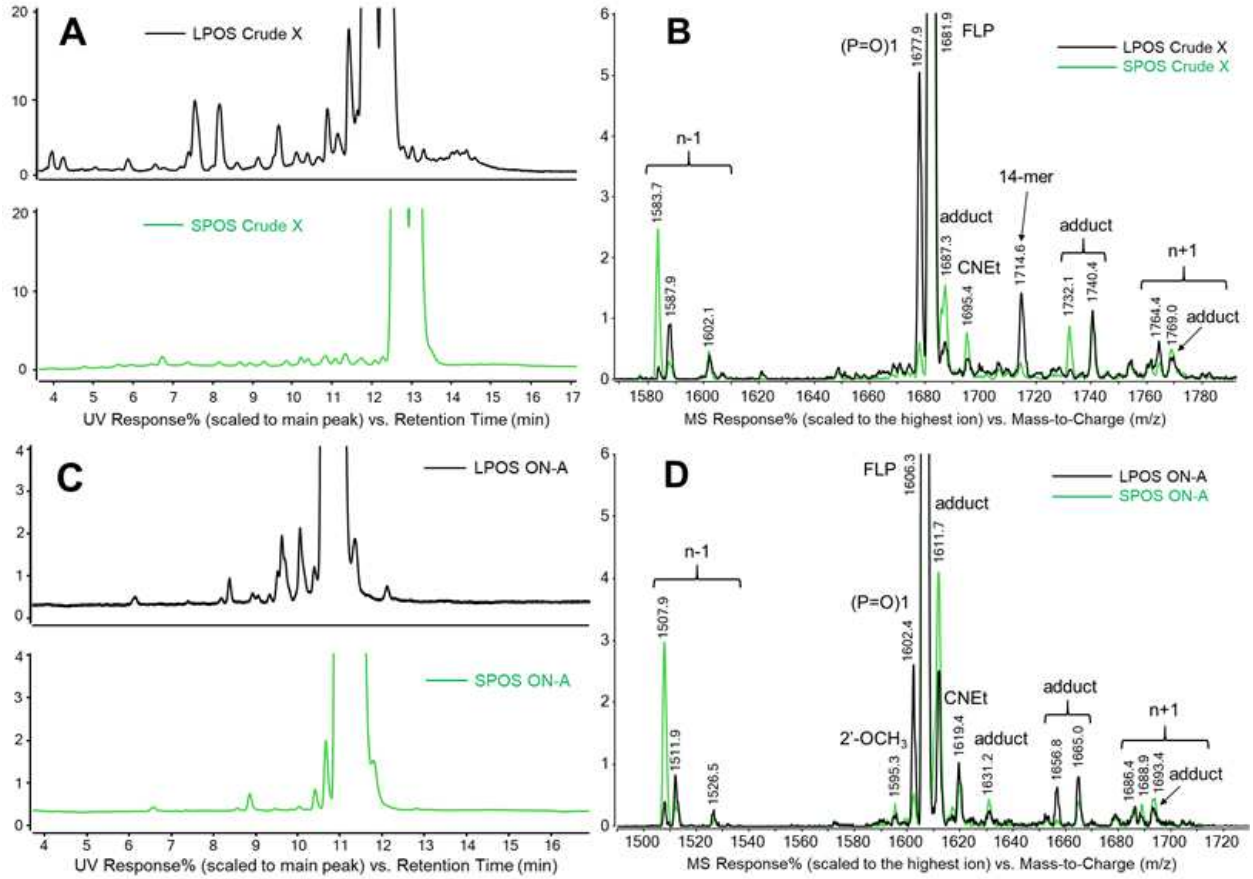

Figure 6. The Impurities of the crude X and ON-A. Black for LPOS and Green for SPOS. **A**. UV chromatograms of **X** from LPOS and SPOS. **B**. MS spectra overlay for **X** from LPOS and SPOS. **C**. UV chromatograms of purified **ON-A** from LPOS and SPOS. **D**. MS spectra overlay for purified **ON-A** from LPOS and SPOS.

purity than SPOS due to the presence of additional shorter and longer retention time impurities (Fig 6A). Among the critical impurities coeluting with **X**, PO (~ 4%) was the only one that was higher in the LPOS material (Fig 6B). Since there are 15 total PS linkages in **X**, the 4.0% PO impurities in the LPOS may consist of 15 isomeric impurities each at ~ 0.26%. PO impurities in LPOS can come from starting material fragments, be formed when linking fragments during convergent assembly and from side reactions during ammonolysis.[39] The impurity profiles of **ON-**

A from LPOS and SPOS after HIC and AEX purification are comparable (Fig. 6C and 6D), demonstrating that the impurities originating from the convergent synthesis were effectively removed by the downstream purification process. The purity of **ON-A** from both SPOS (92.4%) and LPOS (91.4%) is high. The PO impurities from the LPOS were reduced from 4.0% to 2.2% by the AEX chromatography. Total n-1 impurities were found to be lower in the LPOS (1.2%) vs. SPOS (2.9%). This can be attributed to impurity control at the fragment stage. The ions labeled as "adduct" in Fig. 6B and 6D are common artifacts of the ion-pair reversed phase LC-MS analysis and do not represent covalent modification of the **ON-A**. Except for PO, the sum of the levels of the other critical impurities in the four fragments is roughly the same as the total critical impurities observed in crude **X**.

Conclusion

The first convergent synthesis of a therapeutic 18-mer mixed backbone (PO/PS) 2'-MOE gapmer oligonucleotide drug candidate was completed. Control of the hydrolytic substitutions of N^4-NHBz of ^{Me}C nucleotides and essentially quantitative chain extension reactions gave individual tetramer and pentamer fragments in high yields and purities. The total synthesis, with the longest linear path including 9 isolations and 14 reactions is practical and scalable. Syntheses of **II** and **VI** were completed at ~3 kg scale and details of the optimization and scale-up will be reported in the future. Building upon this strategy the late stages of completing the convergent synthesis of a second 18-mer oligonucleotide is in progress and future efforts are focused on exploiting economies of scale as well as decreasing the environmental impact of oligonucleotide manufacturing by streamlining reaction conditions, reducing reagent use and simplifying downstream purification.

References

1. Wang, F., Zuroske, T. & Watts, J.K. RNA therapeutics on the rise. *Nat Rev Drug Discov* (2020).
2. Shi, X. & Tong, C.C. Current State of Oligonucleotide Therapeutics. *Pharmaceutical Engineering* (2020).
3. Lam, J.K., Chow, M.Y., Zhang, Y. & Leung, S.W. siRNA Versus miRNA as Therapeutics for Gene Silencing. *Mol Ther Nucleic Acids* **4**, e252 (2015).
4. Shen, X. & Corey, D.R. Chemistry, Mechanism and Clinical Status of Antisense Oligonucleotides and Duplex RNAs. *Nucleic Acids Research* **46**, 1584-1600 (2018).
5. Khvorova, A. & Watts, J.K. The chemical evolution of oligonucleotide therapies of clinical utility. *Nat Biotechnol* **35**, 238-248 (2017).
6. (Biospace, 2020).
7. Paredes, E. & Konishi, T. Large-Scale Oligonucleotide Manufacturing. (Springer, Singapore; 2018).
8. Cedillo, I. in Euro Tides (RAI Amsterdam, Netherlands.
9. Andrews, B.I. et al. Sustainability Challenges and Opportunities in Oligonucleotide Manufacturing. *J Org Chem* **86**, 49-61 (2021).
10. Molina, A.G. & Sanghvi, Y.S. Liquid-Phase Oligonucleotide Synthesis: Past, Present, and Future Predictions. *Curr Protoc Nucleic Acid Chem* **77**, e82 (2019).
11. Kim, J.F. et al. Organic Solvent Nanofiltration (OSN): A New Technology Platform for Liquid-Phase Oligonucleotide Synthesis (LPOS). *Org. Process Res. Dev.* **20**, 1439-1452 (2016).
12. Chen, C.-H. et al. Convergent Solution Phase Synthesis of Chimeric Oligonucleotides by 2+2 and 3+3 phosphoramidite Strategy. *Aust. J. Chem.* **63**, 227-235 (2010).
13. Brown, J.M., Christodoulou, C., Modak, A.S., Reese, C.B. & Serafinowska, H.T. Synthesis of the 3′-terminal half of yeast alanine transfer ribonucleic acid (tRNAAla) by the phosphotriester approach in solution. Part 2. *J Chem Soc, Perkin Trans 1*, 1751-1767 (1989).
14. Reese, C.B. & Yan, H. Solution phase synthesis of ISIS 2922 (Vitravene) by the modified H-phosphonate approach. *J Chem Soc, Perkin Trans 1*, 2733-2903 (2002).
15. Tew, D. in TIDES US (San Diego, USA; 2019).
16. Takahashi, D. in TIDES US Nov 12-15, 2019 (Boston, MA, USA; 2020).
17. Eckstein, F. Phosphorothioates, essential components of therapeutic oligonucleotides. *Nucleic Acid Ther* **24**, 374-387 (2014).
18. Grajkowski, A., Cieslak, J. & Beaucage, S.L. Solid-Phase Purification of Synthetic DNA Sequences. *J Org Chem* **81**, 6165-6175 (2016).
19. Kim, S., Matsumoto, M. & Chiba, K. Liquid-phase RNA synthesis by using alkyl-chain-soluble support. *Chemistry* **19**, 8615-8620 (2013).
20. Pourshahian, S. Therapeutic Oligonucleotides, Impurities, Degradants, and Their Characterization by Mass Spectrometry. *Mass Spectrom Rev* **40**, 75-109 (2019).
21. Capaldi, D. et al. Impurities in Oligonucleotide Drug Substances and Drug Products. *Nucleic Acid Ther* **27**, 309-322 (2017).
22. Goyon, A., Yehl, P. & Zhang, K. Characterization of therapeutic oligonucleotides by liquid chromatography. *J Pharm Biomed Anal* **182**, 113105 (2020).
23. Scozzari, A.N. & Capaldi, D.C. in Antisense Drug Technology Principles, Strategies, and Applications, Second Edition, Edn. 2nd 401-434 (CRC Press, Boca Raton; 2007).
24. Yang, J. et al. Solid-Phase Synthesis of Phosphorothioate Oligonucleotides Using Sulfurization Byproducts for in Situ Capping. *J Org Chem* **83**, 11577-11585 (2018).
25. Bonora, G.M. et al. A Liquid-Phase Process Suitable for Large-Scale Synthesis of Phosphorothioate Oligonucleotides. *Org. Proc. Res. Dev.* **4**, 225-231 (2000).
26. Koning, M.C.D., Ghisaidoobe, A.B.T., Duynstee, H.I., Kortenaar, P.B.W.T. & Filippov, D.V.M., G. A. van der Simple and Efficient Solution-Phase Synthesis of Oligonucleotides Using Extractive Work-Up. *Org. Proc. Res. Dev.* **10** 1238–1245 (2006).
27. Molina, A.G., Kungurtsev, V., Virta, P. & Lonnberg, H. Acetylated and methylated beta-cyclodextrins as viable soluble supports for the synthesis of short 2'-oligodeoxyribo-nucleotides in solution. *Molecules* **17**, 12102-12120 (2012).
28. Creusen, G., Akintayo, C.O., Schumann, K. & Walther, A. Scalable One-Pot-Liquid-Phase Oligonucleotide Synthesis for Model Network Hydrogels. *J Am Chem Soc* **142**, 16610-16621 (2020).
29. Katayama, S. & Hirai, K. Liquid-Phase Synthesis of Oligonucleotides. (Springer, Singapore; 2018).

30. Ravikumar, V.T. & Cole, D.L. Development of 2'-O-Methoxyethyl Phosphorothioate Oligonucleotides as Antisense Drugs under Stereochemical Control. *Org. Proc. Res. Dev.* **6**, 798-806 (2002).
31. Featherston, A.L. et al. Catalytic asymmetric and stereodivergent oligonucleotide synthesis. *Science* **371**, 702-707 (2021).
32. Jahns, H. et al. Stereochemical bias introduced during RNA synthesis modulates the activity of phosphorothioate siRNAs. *Nat Commun* **6**, 6317 (2015).
33. More discussion regarding the classification of impurities in fragment starting materials can be found in W. F. Kiesman et al., Perspectives on the Designation of Oligonucleotide Starting Materials. Nucleic Acid Ther, (2021).
34. Nowak, I. & Robins, M.J. Hydrothermal deamidation of 4-N-acylcytosine nucleoside derivatives: efficient synthesis of uracil nucleoside esters. *Org Lett* **7**, 4903-4905 (2005).
35. Holy, A. Acid-catalyzed migration of N4-acyl groups in cytosine derivatives. *Collect. Czech. Chem. Commun.* **44**, 1819-1827 (1979).
36. Gaffney, B.L., Veliath, E., Zhao, J. & Jones, R.A. One-flask syntheses of c-di-GMP and the [Rp,Rp] and [Rp,Sp] thiophosphate analogues. *Org Lett* **12**, 3269-3271 (2010).
37. Singh, A. et al. Solution-phase synthesis of branched DNA hybrids via H-phosphonate dimers. *J Org Chem* **77**, 2718-2728 (2012).
38. For analysis of deamination impurities in oligonucleotides, see C. Rentel et al., Determination of oligonucleotide deamination by high resolution mass spectrometry. J Pharm Biomed Anal 173, 56-61 (2019).
39. Kodra, J.T., Kehler, J. & Dahl, O. Stability of oligodeoxynucleoside phosphorodithioates and phosphorothioates in aqueous ammonia. *Nucleic Acids Res* **23**, 3349-3350 (1995).

Methods

Detailed experimental and analytical procedures and data are available in the supplementary materials.

Data and materials availability

Detailed experimental and analytical procedures and data are available in the supplementary materials.

Acknowledgements

The authors would like to thank our Biogen colleagues, Ms. Hein Nguyen for purification support, Drs. William Zhang and Rasika Phansalkar for sample analysis, Drs. Jess Stolee, Lou Coury, Don Walker of Biogen and Daniel Capaldi of Ionis Pharmaceuticals for their review of this manuscript, and the chemists at Pharmaron (Beijing), Wuxi CSU (Tianjin) and Wuxi STA (Changzhou) for their contributions in the development of the process.

Author contributions

X.S., W.F.K. and F.D.A. conceived of the project. X.Z, W.Y., Y.A.F., L.X., A.D., R.S.G designed and performed the experiments. H.J. and J.Y. analyzed the data. W.F.K and X.S. wrote the manuscript.

Competing interests

All authors are employed by and own stock in Biogen, Inc.

Supplementary Files

This is a list of supplementary files associated with this preprint. Click to download.

- SupplementaryMaterialNatureCommunications.pdf
- SupplementaryMaterialpartIIProcedurefor3kgsynthesisofVIandII.pdf